Experimental and Theoretical Studies of Olefin Insertion for *ansa*-Niobocene and *ansa*-Tantalocene Ethylene Hydride Complexes

Lily J. Ackerman,[†] Malcolm L. H. Green,[‡] Jennifer C. Green,[‡] and John E. Bercaw*,[†]

Arnold and Mabel Beckman Laboratories of Chemical Synthesis, California Institute of Technology, Pasadena, California 91125, and Inorganic Chemistry Laboratory, South Parks Road, Oxford University, Oxford OX1 3QR, U.K.

Received August 2, 2002

Using dynamic NMR methods the rates of hydrogen exchange following intramolecular ethylene insertion into the metal−hydride bond have been measured for the following group 5 *ansa*-metallocene complexes: $[Me_2Si(\eta^5\text{-}C_5H_4)(\eta^5\text{-}C_5H_3\text{-}3\text{-}R)]Nb(CH_2CH_2)H$ (R = $CHMe_2$, CMe_3), *rac*- and *meso*-$[Me_2Si(\eta^5\text{-}C_5H_3\text{-}3\text{-}CMe_3)_2]Nb(CH_2CH_2)H$, and $[(1,2\text{-}SiMe_2)_2(\eta^5\text{-}C_5H\text{-}3,5\text{-}(CHMe_2)_2)(\eta^5\text{-}C_5H_2\text{-}4\text{-}CMe_3)]Ta(CH_2CH_2)H$. The singly bridged *ansa*-niobocenes exchange up to 3 orders of magnitude faster than unbridged complexes. However, the doubly bridged *ansa*-tantalocene complex exchanges at a rate comparable to that previously reported for $(\eta^5\text{-}C_5Me_5)_2Ta(CH_2CH_2)H$ and much slower than a singly bridged complex, $[Me_2Si(\eta^5\text{-}C_5Me_4)_2]Ta(CH_2CH_2)H$. These "*ansa*-effects" were investigated by DFT calculations on model complexes. The computed exchange pathway showed the presence of an agostic ethyl intermediate. The calculated barriers for hydrogen exchange of model unbridged, singly bridged, and doubly bridged niobocenes correlate with the experimental results.

Introduction

Olefin insertion into a metal−hydrogen bond and the microscopic reverse, β-hydrogen elimination, are elementary reactions in organometallic chemistry. These transformations are of considerable interest due to their fundamental importance, as well as for their widespread occurrence in synthetic and catalytic processes. Both reactions occur in transition-metal-catalyzed processes such as olefin polymerization, isomerization, and hydrogenation.[1] Mechanistic studies on the reversible insertion of alkenes into M−H bonds have been carried out for a series of group 5 olefin hydride complexes (Figure 1).[2] These complexes exist between two limiting resonance structures: d^2, M^{III} olefin hydride or d^0, M^V metallocyclopropane hydride (Scheme 1).

Rates of hydrogen exchange following olefin insertion were measured by either magnetization transfer or coalescence ^1H NMR techniques. The study revealed that the insertion step proceeds via a four-centered transition state with modest charge development:

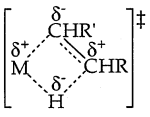

Thus, the transition state is stabilized when R is electron donating and R′ is electron withdrawing. On the other hand, the ground-state olefin hydride complex is stabilized when both R and R′ are electron withdrawing, due to stronger π-back-bonding interactions. The ground state is also stabilized for tantalum relative to niobium. This can be understood if the insertion process is viewed as a reductive elimination of a C−H bond for the M^V, d^0 resonance structure, since higher oxidation states are generally preferred by the heavier congener of a periodic triad. Thus, the observed order of elimination rates is $k_{ins}(Nb) > k_{ins}(Ta)$.

When comparing the effect of ancillary ligands on the rate of insertion, one would expect the more electron-donating pentamethylcyclopentadienyl ligands (Cp*) to stabilize the M^V-like ground state relative to the M^{III}-

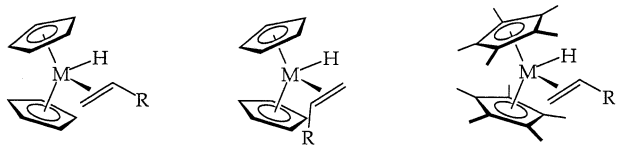

M = Nb; R = H, CH_3, Ph, C_6H_4-*m*-X, C_6H_4-*p*-X (X = CF_3, CH_3, OMe, NMe_2).
M = Ta; R = H, CH_3.

Figure 1. Group 5 olefin hydride complexes previously utilized to investigate olefin insertion into the M−H bond.

Scheme 1

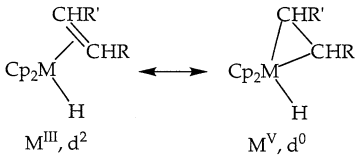

[†] California Institute of Technology.
[‡] Oxford University.

(1) Parshall, G. W.; Ittel, S. D. *Homogeneous Catalysis*, 2nd ed.; Wiley: New York, 1992; Chapters 2−4.

(2) (a) Doherty, N. M.; Bercaw, J. E. *J. Am. Chem. Soc.* **1985**, *107*, 2670−2682. (b) Burger, B. J.; Santarsiero, B. D.; Trimmer, M. S.; Bercaw, J. E. *J. Am. Chem. Soc.* **1988**, *110*, 3134−3146.

10.1021/om0206296 CCC: $25.00
Publication on Web 12/07/2002

Table 1. Activation Barriers for Olefin Insertion of Selected Complexes[2]

complex	$\Delta G^{\ddagger}$ (50 °C, kcal mol^{-1})
$Cp^*_2Nb(CH_2CH_2)(H)$	18.3(1)
$Cp_2Nb(CH_2CH_2)(H)$	17.1(1)
$Cp^*_2Nb(CH_2CHCH_3)(H)$	14.6(1)
$Cp_2Nb(CH_2CHCH_3)(H)$	16.5(1)
$Cp^*_2Nb(CH_2CHPh)(H)$	18.3(1)
$Cp_2Nb(CH_2CHPh)(H)$	20.5(1)

like transition state. However, the Cp* ligands would have the opposite effect sterically, as they would destabilize the congested ground state relative to the less crowded transition state. The activation barriers for representative complexes are summarized in Table 1. For the ethylene hydride complexes, $\Delta G^{\ddagger}(Cp^*) > \Delta G^{\ddagger}(Cp)$; thus, electronic effects dominate for the smallest olefin ligand. However, sterics dominate for larger olefins (propylene, styrene), since $\Delta G^{\ddagger}(Cp^*) < \Delta G^{\ddagger}(Cp)$.

ansa-Metallocenes (Chart 1) have attracted much interest in Ziegler−Natta catalysis due to recent success in the development of stereospecific polymerization catalysts by strategic placement of substituents on the rigid *ansa*-metallocene fragment.[3−5] *ansa*-Metallocene complexes are also used as enantioselective catalysts for C−C and C−H bond formation.[6] More recently, doubly bridged *ansa*-metallocenes have been prepared and are among the most active catalysts for the syndiospecific polymerization of propylene (Chart 1).[7] Thus, the investigation of ansa complexes in comparison with their nonbridged counterparts has been an active area of research.

Studies have revealed that in some cases the reactivity of an ansa complex is substantially different than that of an unbridged analogue. For example, the thermal stability of $[Me_2C(\eta^5\text{-}C_5H_4)_2]W(CH_3)H$ is much greater than that of $(\eta^5\text{-}C_5H_5)_2W(CH_3)H$.[8] The ansa complex is stable to reductive elimination of methane under thermal and photochemical conditions (up to 120 °C), but the unbridged complex loses methane at ca. 50 °C. A theoretical study by Jardine and Green revealed that after reductive elimination from the singlet methane σ complex $\{(\eta^5\text{-}C_5H_5)_2W(CH_4)\}$ the proposed 16-electron intermediate $\{(\eta^5\text{-}C_5H_5)_2W\}$ is able to relax to a low-energy, parallel ring triplet state, facilitating methane loss.[9] However, the ansa bridge constrains the rings, raising the triplet ground state of the intermediate such that little energy gain is possible upon methane loss. Other explanations have been proposed for the differing reactivity that the ansa bridge imparts in related metallocene systems. For example, Parkin has shown that the barrier to PMe_3 dissociation for $[Me_2Si(\eta^5\text{-}C_5Me_4)_2]ZrH_2(PMe_3)$ is much larger than that for $Cp^*_2ZrH_2(PMe_3)$, with $k_{Cp^*} > 500k_{ansa}$ at 25 °C.[10] Shin and Parkin have also reported that the rate of olefin insertion for $[Me_2Si(C_5Me_4)_2]Ta(CH_2CH_2)H$ is 3 orders of magnitude faster than that for the corresponding unbridged complex $Cp^*_2Ta(CH_2CH_2)H$.[11] These authors argue that the singly bridged ansa ligand is less electron donating than the unconstrained cyclopentadienyl ligands, resulting in a more electrophilic metal center. Hence, the zirconium center binds PMe_3 more tightly in the ansa complex. Similarly, the tantalum center back-bonds to the olefin π^* orbital less efficiently for $[Me_2Si(C_5Me_4)_2]Ta(CH_2CH_2)H$; the ground state is destablized, and insertion is faster.

In this study, further investigations of ansa effects on olefin insertion have been undertaken by synthesizing and measuring hydrogen exchange rates for group 5 *ansa*-metallocene ethylene hydride compounds. Substitution patterns and the effects of introducing a second linking group for *ansa*-metallocene olefin hydride complexes have been investigated. DFT calculations have also been performed on model complexes.

Chart 1

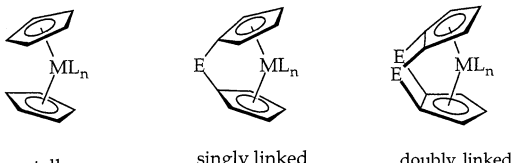

metallocene | singly linked *ansa*-metallocene | doubly linked *ansa*-metallocene

(E = CH_2, CMe_2, CPh_2, $SiMe_2$, C_2H_4)

Chart 2

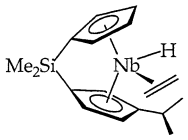

(1) iPrSpNb(CH_2CH_2)H

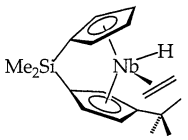

(2) tBuSpNb(CH_2CH_2)H

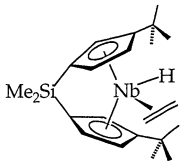

(3) *meso*-DpNb(CH_2CH_2)H

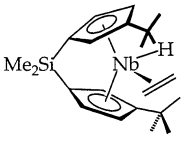

(4) *rac*-DpNb(CH_2CH_2)H

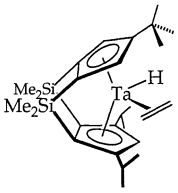

(5) tBuThpTa(CH_2CH_2)H

Results and Discussion

Measurement of Hydrogen Exchange Rates. The *ansa*-niobocene and -tantalocene ethylene hydride complexes prepared for this study are shown in Chart 2. The synthesis and characterization (NMR, X-ray) of the

(3) Brintzinger, H. H.; Fischer, D.; Müllhaupt, R.; Rieger, B.; Waymouth, R. M. *Angew. Chem., Int. Ed. Engl.* **1995**, *34*, 1143−1170.
(4) Kaminsky, W.; Kullper, K.; Brintzinger, H. H.; Wild, F. R. W. P. *Angew. Chem., Int. Ed. Engl.* **1985**, *24*, 507−508.
(5) Ewen, J. A.; Jones, R. L.; Razavi, A.; Ferrara, J. D. *J. Am. Chem. Soc.* **1988**, *110*, 6255−6256.
(6) Hoveyda, A. H.; Morken, J. P. *Angew. Chem., Int. Ed. Engl.* **1996**, *35*, 1262−1284.
(7) Herzog, T. A.; Zubris, D. L.; Bercaw, J. E. *J. Am. Chem. Soc.* **1996**, *118*, 11988−11989.
(8) Labella, L.; Chernega, A.; Green, M. L. H. *J. Chem. Soc., Dalton Trans.* **1995**, 395−402.
(9) Jardine, C. N.; Green, J. C. *J. Chem. Soc., Dalton Trans.* **1998**, 1057−1061.
(10) Lee, H.; Desrosiers, P. J.; Guzei, I.; Rheingold, A. L.; Parkin, G. *J. Am. Chem. Soc.* **1998**, *120*, 3255−3256.
(11) Shin, J. H.; Parkin, G. *Chem. Commun.* **1999**, 887−888.

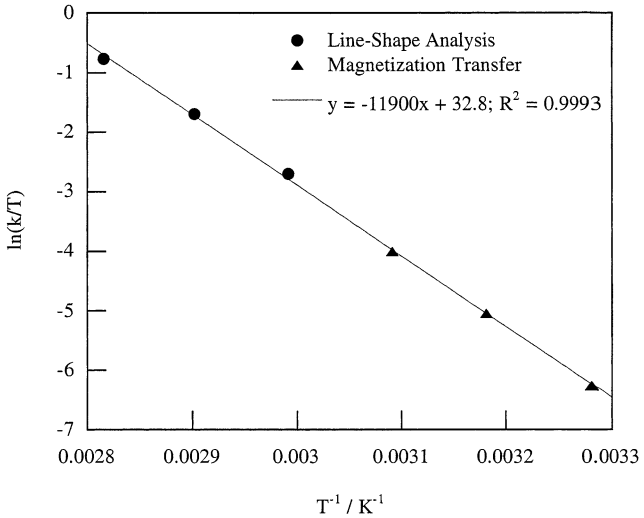

Figure 2. Eyring plot for endo methylene hydrogen/hydride exchange for complex **3** utilizing two different NMR methods: magnetization transfer and line-shape analysis.

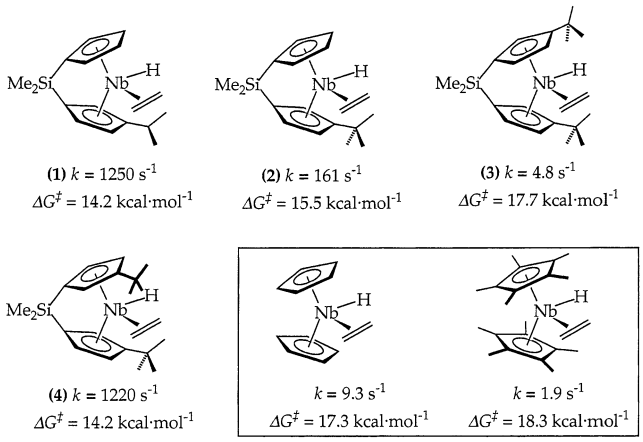

Figure 3. Olefin insertion rates and free energy barriers at 318 K for various niobocene ethylene hydride complexes. Rates for unbridged complexes (in box) have been reported in ref 2.

complexes are reported elsewhere.[12] All complexes exhibit fluxional behavior observable by variable-temperature NMR due to olefin insertion into the M−H bond and subsequent β-hydrogen elimination. Rates for this overall hydrogen exchange process upon ethylene insertion, C−C bond rotation for the ethyl product, and β-hydrogen elimination were determined by ^{1}H NMR line-shape analysis (all complexes) or magnetization transfer (complex **3**). The temperature-dependent broadening of the hydride resonance was used to calculate exchange rates in the line-shape simulations, assuming that the hydrogens become equivalent after insertion to form the ethyl complex. Magnetization transfer analysis was most suitable for **3**, since the complex is C_s symmetric, and the (equivalent) endo hydrogens undergoing exchange give rise to a well-defined triplet in the ^{1}H spectrum. On the other hand, analysis of magnetization transfer data for **1**, **2**, and **4** is complicated by the close proximity of the inequivalent endo hydrogens undergoing exchange and the complicated coupling patterns in these C_1-symmetric niobocenes.[13,14] Also, the endo and exo CH_2═CH_2 resonances are not well resolved for complex **5**. Nevertheless, the line-shape analysis data correlate well with magnetization transfer data for complex **3**, providing an independent check on the method (Figure 2).

Hydrogen exchange rate constants and free energies of activation at 318 K for *ansa*-niobocene complexes **1**−**4**, together with those for the previously studied complexes (η^5-C_5H_5)$_2$Nb(CH_2CH_2)H and (η^5-C_5Me_5)$_2$Nb(CH_2CH_2)H for comparison, are presented in Figure 3.[2] In agreement with Parkin's results for the *ansa*-tantalocene system (vide supra), the ansa ligand array appears to lower the activation barrier for hydrogen exchange compared to that for the unbridged complexes (complexes **1**, **2**, and **4**).[11] Although a direct comparison of (η^5-C_5H_5)$_2$Nb(CH_2CH_2)H to [Me_2Si(η^5-C_5H_4)$_2$]Nb(CH_2-CH_2)H is lacking, there appear to be large ansa effects on the rates of hydrogen exchange, as evidenced by the greater than 2 order rate increase for **1** vs (η^5-C_5H_5)$_2$-Nb(CH_2CH_2)H. Less electron donation for a singly [$SiMe_2$]-bridged ligand relative to an unlinked analogue has been attributed to pulling of the cyclopentadienyl rings back toward η^3:η^3 hapticity.[10,11] More recently, infrared, electrochemical and DFT studies for a large number of zirconocene complexes have been undertaken to probe the effect of introducing single and double ansa linkages to the parent unlinked system.[15] These studies revealed lower electron density at the metal center for singly bridged metallocene fragments. By extension, the d^2 metal center of the [Me_2Si(η^5-C_5H_4)$_2$]Nb(CH_2CH_2)H is expected to be less electron rich, and the ground state is electronically destabilized relative to (η^5-C_5H_5)$_2$Nb-(CH_2CH_2)H.

That there are specific steric interactions influencing hydrogen exchange is evident from the decrease in rates going from **1** to **2** but, most strikingly, by the large difference in exchange rates for **3** and **4**. The racemic complex **4** is among the fastest to undergo exchange, whereas the meso complex **3** exchanges on the same time scale as the unbridged complexes. This difference in rates for **3** and **4** can be attributed solely to steric placement of the *tert*-butyl groups, since the complexes are essentially identical electronically. Increasing the steric bulk from isopropyl (**1**) to one or two *tert*-butyl groups (**2**, **3**) on one side of the metallocene wedge successively decreases the rate of exchange, culminating with the drastically slower exchange rate observed for **3**. We postulate that the preference for ethylene to reside on the side of the niobocene wedge away from the isopropyl or *tert*-butyl group(s) is steric in origin and that the insertion transition structures that necessarily move the ethylene toward the hydride ligand on the

(12) Chirik, P. J.; Zubris, D. L.; Ackerman, L. J.; Henling, L. M.; Day, M. W.; Bercaw, J. E. *Organometallics* **2003**, *22*, 172−187.

(13) Magnetization transfer experiments were attempted for complex **1**, but the data could not be fitted within reasonable error limits.

(14) Typically, the magnetization transfer experiment is utilized to measure exchange between uncoupled protons (singlets in the ^{1}H spectrum). However, if the coupling is small compared to the chemical shift separation of the exchanging resonances (which is the case for **3**, but not for **1**, **2**, and **4**), the magnetization transfer experiment can provide meaningful rate data.[2] For more details on this subject see: Doherty, N. M. Ph.D. Thesis, California Institute of Technology, Appendix I, 1984, and references therein.

(15) (a) Zachmanoglou, C.; Docrat, A.; Bridgewater, B. M.; Parkin, G.; Brandow, C. G.; Bercaw, J. E.; Jardine, C. N.; Lyall, M.; Green, J. C.; Keister, J. *J. Am. Chem. Soc.* **2002**, *124*, 9525−9546. (b) Brandow, C. G. Ph.D. Thesis, California Institute of Technology, 2001. (c) Jardine, C. N. Ph.D. Thesis, St. Catherine's College, Oxford University, 2000.

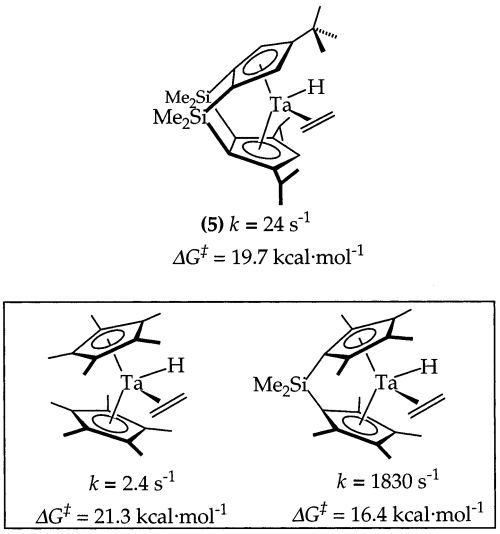

Figure 4. Olefin insertion rates and free energy barriers at 373 K for various tantalocene ethylene hydride complexes. Rates for complexes (in box) have been reported in refs 2b and 11, respectively.

other side are increasingly crowded on going from **1** with one isopropyl substituent to **2** with one *tert*-butyl substituent to **3** with two *tert*-butyl substituents. The ethylene hydride complex **4** has more steric crowding than **1**, **2**, or **3**, since the *rac* isomer necessarily possesses a close *tert*-butyl/ethylene interaction. Thus, the ground state is destablized and the barrier for insertion is substantially reduced from that for **3**. Large steric effects have also been observed for the insertion of olefins into neutral group 4 zirconocene dihydrides.[16]

The doubly [$SiMe_2$]-bridged *ansa*-tantalocene complex **5** was found to exchange at a rate more comparable to unlinked (η^5-$C_5Me_5)_2Ta(CH_2CH_2)H$ than to the singly [$SiMe_2$]-bridged *ansa*-tantalocene complex [$Me_2Si(\eta^5$-$C_5Me_4)_2$]$Ta(CH_2CH_2)H$ (Figure 4). At first sight it would appear puzzling that double linking of the cyclopentadienyl ligands has the net effect of unlinking them! Crystallographic data for (η^5-$C_5H_5)_2ZrCl_2$, [$Me_2Si(\eta^5$-$C_5H_4)_2$}$ZrCl_2$, and [$(Me_2Si)_2(\eta^5$-$C_5H_3)_2$]$ZrCl_2$ show that the Cp_{cent}−Zr−Cp_{cent} angles decrease and the range of Zr−C bond lengths increases in a smooth progression as ansa linkages are introduced.[15a] With regard to the electronic effects of doubly linking the cyclopentadienyl ligands, these recent investigations indicated that the electron-donating effect of two vicinal [Me_2Si] ansa bridges in combination with a ligand conformation with an "η^2-ene-allyl" type coordination mode reduces back-donation from the metal to the cyclopentadienyl ligands.[15a] Hence, the d^2 metal center of [(1,2-$SiMe_2)_2(\eta^5$-C_5H-3,5-$(CHMe_2)_2)(\eta^5$-C_5H_2-4-$CMe_3)$]$Ta(CH_2CH_2)H$ is approximately as good a π donor, and the ground state is expected to be similar to (η^5-$C_5Me_5)_2Ta(CH_2CH_2)H$.

Density Functional Calculations. To increase understanding of the effect of single and double ansa bridges on the hydrogen exchange rate, density functional calculations were carried out on model systems, [$Cp^R_2Nb(C_2H_4)H$], where $Cp^R_2 = (\eta^5$-$C_5H_5)_2$ (**6**), [$H_2Si(\eta^5$-$C_5H_4)_2$] (**7**), and $(H_2Si)_2(\eta^5$-$C_5H_3)_2$ (**8**) (Chart 3). Four stationary points were identified on the hydrogen

Chart 3

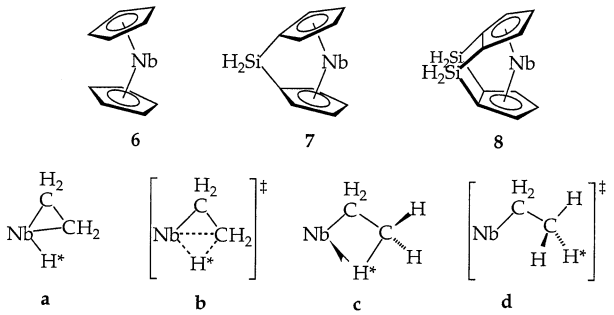

exchange surface for model complexes **6**−**8**: the ethylene hydride complex $Cp^R_2Nb(\eta^2$-$C_2H_4)H$ (**a**), the β-agostic ethyl complex $Cp^R_2Nb(\eta^2$-$C_2H_5)$ (**c**), an insertion transition state between these two minima (**b**), and the transition state for dissociation of the β-C−H bond (**d**) (Chart 3).

Full geometry optimizations were carried out on all stationary points, and frequency calculations showed **a** and **c** to be local minima, having only positive frequencies, and **b** and **d** to be transition states, each having only one imaginary frequency. Energies relative to Cp^R_2-$Nb(\eta^2$-$C_2H_4)H$ and key geometric parameters are given in Table 2.

Table 2. Energies (kcal mol^{-1}) and Selected Bond Lengths (Å) and Angles (deg) for 6−8

	energy	Nb−H	C_{endo}−H	C−C	Nb−C_{exo}	inter-ring angle
6a	0	1.757	2.320	1.434	2.338	43
7a	0	1.765	2.332	1.427	2.344	54
8a	0	1.762	2.313	1.431	2.333	61
6b	12.45	1.814	1.430	1.466	2.299	38
7b	9.22	1.809	1.573	1.448	2.317	53
8b	12.68	1.881	1.385	1.478	2.281	58
6c	10.61	1.976	1.205	1.504	2.278	47
7c	6.46	1.988	1.200	1.503	2.268	53
8c	10.61	2.005	1.193	1.509	2.263	59
6d	18.91	2.856	1.105	1.543	2.265	48
7d	14.30	2.766	1.107	1.540	2.248	54
8d	17.30	2.681	1.110	1.534	2.249	60

Ground-State Structures. For all three ethylene hydride complexes **6a**−**8a**, the Nb−H bond length is ca. 1.76 Å and the long C−C bond for the coordinated ethylene is around 1.43 Å. This latter value is in good agreement with the crystal structure of complex **2**, which has a C−C distance of 1.41 Å.[12] Such a bond length implies considerable back-donation to the olefin and an approach to a metallocyclopropane structure. The β-agostic ethyl structures **c** have very stretched agostic C−H bonds, ca. 1.2 Å, with the C−C bonds lengthened to around 1.50 Å. The Nb−H distances are consistent with agostic bonding at 1.98−2.01 Å. With a 60° rotation about the C−C bond, the exchanging hydrogens become equivalent at the transition states **d**, which have normal ethyl groups with C−H bond lengths of 1.105−1.110 Å and C−C bond lengths ranging between 1.534 and 1.543 Å. The Nb−H contacts for **d** are now long, being greater than 2.6 Å. The greatest differences between the systems are calculated for the insertion transition states **b**, which, on distance criteria, appear to be earliest for **7** and latest for **8**. The relative cyclopentadienyl ring orientations are fixed for **7** and **8**, constrained by their respective bridges, and the variation in inter-ring angle is small as one follows the reaction progression from **a** to **d**. However, for **6** the

(16) Chirik, P. J. Ph.D. Thesis, California Institute of Technology, 2000.

Chart 4

4-carbon front face — 2-carbon front face

7 8

rings are closer to being eclipsed than staggered. The unlinked **6a** and **6b** have a two-carbon front face conformation, as in **8**, but for **6c** and **6d**, the rings reorient to give a four-carbon front face conformation, as in **7** (Chart 4).[15a]

Mechanism for Hydrogen Exchange. Relative energies, given in Table 2 and represented diagrammatically in Scheme 2, concur well with the experimental values and trends, showing a significantly lower activation energy for the singly bridged system **7**. The agostic ethyl **c** is lower in energy for **7** than for **6** or **8** (which fortuitously are calculated to have the same energy). As the insertion barrier and exchange barrier are also lower for **7**, this is consistent with faster exchange rates measured for singly linked compounds. The energy differences between the agostic ethyl **c** and the transition state **d** are 2.0 kcal mol^{-1} for **6**, 1.9 kcal mol^{-1} for **7**, and 1.6 kcal mol^{-1} for **8**. Complex **8d** shows marginally longer C−H bonds, and shorter Nb−H distances, suggesting that the transition state may maintain a very weak interaction between the exchanging hydrogens and the metal; however, for all three **d** is best described as a nonagostic ethyl. For all three systems a significant portion of the barrier to hydrogen exchange comes from the barrier to rotation of the methyl groups.

In previous studies of olefin insertion into group 5 metal−hydride bonds it has been assumed that, after the olefin inserts, there is a lower barrier to rotation about the C−C bond which exchanges the hydrogens, followed by fast β-hydrogen elimination. An agostic interaction may or may not be cleaved following the insertion step to exchange the hydrogens (Scheme 3). The density functional calculations of this work support the formation and cleavage of a β-agostic structure to exchange the hydrogen atoms after the insertion event. Our research groups had earlier suggested that an "in-place" rotation mechanism will exchange hydrogen atoms after propene or ethylene insertion into a metal−hydride bond.[17] After insertion, the propyl or ethyl intermediate retains agostic bonding to the metal center while the hydrogens undergoing exchange rotate. Our calculations do not support this mechanism (except possibly for complex **8** (vide supra)) but suggest that upon C−C bond rotation the agostic interaction is completely broken. Hydrogen atom exchange can then be observed in the ^{1}H NMR spectrum following β-hydrogen elimination.

When the relative barriers for insertion versus hydrogen atom exchange were compared, it was unexpected that the highest free energy barrier along the reaction profile for hydrogen exchange was methyl rotation (Scheme 2). This conclusion raises questions

Scheme 2

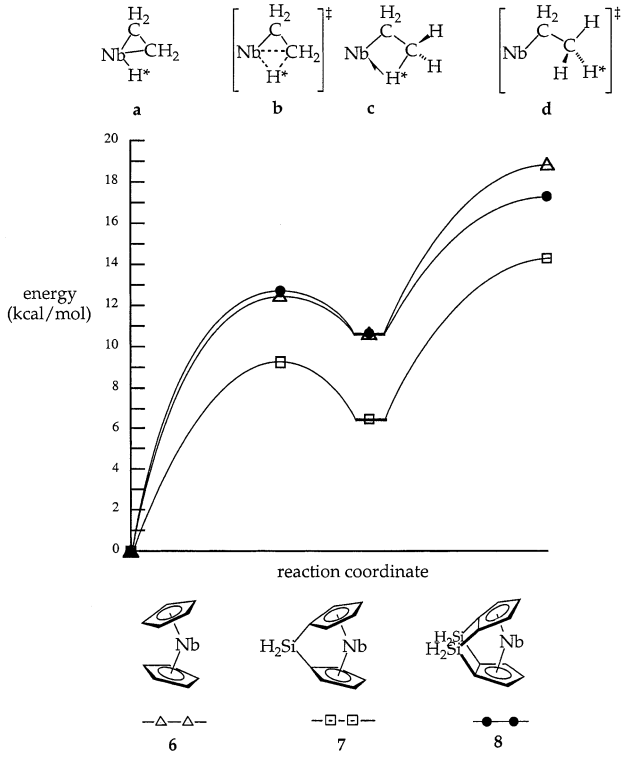

6 7 8

concerning the interpretations of the steric and electronic effects for olefin insertion for this system, since previously the rate-determining step was assumed to be the insertion step.[2] On the other hand, the calculations reveal that the largest differences for **6**−**8** are the barriers for olefin insertion (**b**) and the energies for **c**. The barriers for methyl rotation (**d**) are quite similar for the three systems (with the caveat that the doubly [SiH_2]-bridged ansa complex has a slightly lower barrier, probably due to some weak agostic interactions as it rotates; vide supra). If this trend is general, i.e. the stereoelectronic influences on olefin insertion dominate, and the barriers for alkyl rotation are similar, then the principal conclusions reached from earlier studies are likely still valid.

Experimentally measuring these two separate barriers would be difficult for this group 5 metallocene system. Shultz and Brookhart have been able to measure independently the barriers to C−C bond rotation and β-H elimination for a cationic (diimine)Pd^{II} β-agostic ethyl complex by variable-temperature ^{1}H NMR.[18] For their palladium system the most stable structure is the β-agostic ethyl complex that exhibits three distinct resonances for the α- and β-methylene protons and the agostic proton at low temperatures. Upon warming, coalescence of the α- and β-methylene resonances is observed before the resonance for the agostic β-proton displays any line broadening. Thus, the β-H elimination/olefin rotation/reinsertion process is faster than the C−C bond rotation process for the β-agostic ethyl ground state. Line shape analysis of the resonance for the β-agostic hydrogen at higher temperatures revealed the barrier to C−C bond rotation. At high temperatures, all five resonances coalesce as a result of the combination

(17) (a) Green, M. L. H.; Sella, A.; Wong, L. *Organometallics* **1992**, *11*, 2650−2659. (b) Derome, A. E.; Green, M. L. H.; Wong, L. *New J. Chem.* **1989**, *13*, 747−753.

(18) Shultz, L. H.; Brookhart, M. *Organometallics* **2001**, *20*, 3975−3982.

Scheme 3

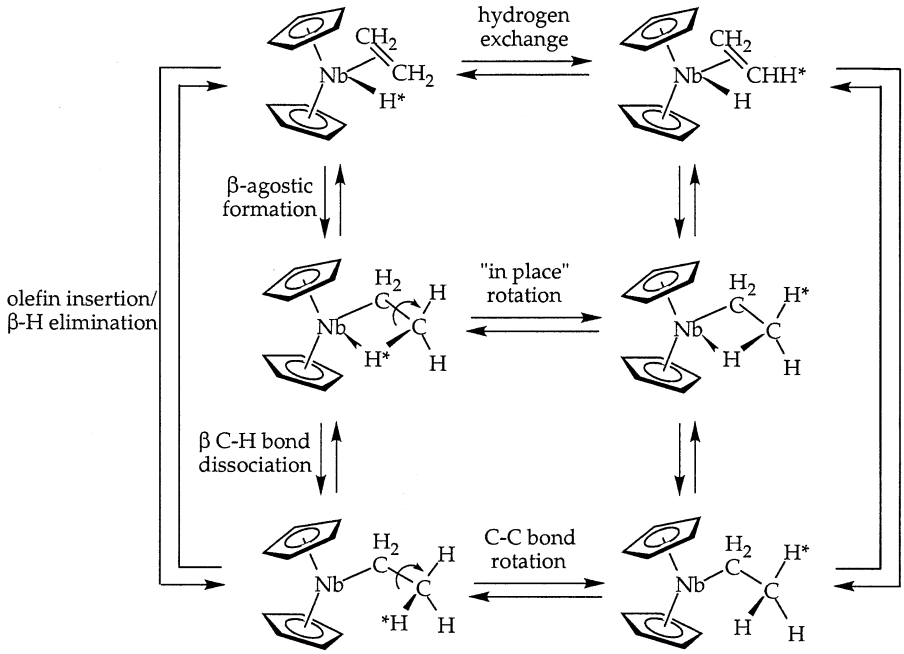

of the two processes. Thus, the barrier for β-H elimination, $\Delta G^{\ddagger}$(165 K), was established as 7.1 kcal mol^{-1} and that for C−C bond rotation, $\Delta G^{\ddagger}$(165 K), as 8.4 kcal mol^{-1}. For the group 5 metallocene ethylene hydride complexes the β-agostic ethyl is *not* the stable structure, and thus, a similar analysis is not possible.

Bonding Considerations. Formally, the formation of the ethyl transition state can be viewed as a reduction from Nb^{V} to Nb^{III}. Fragment analysis of the rotation transition states **d** confirm that these closely resemble a d^2 species where the two metal electrons occupy a d_{x^2} metallocene orbital lying in the metallocene bonding plane. The stability of the analogous orbital in zirconocene compounds has been shown to vary in the order **7** > **6** > **8**;[15a] thus, the relative ease of exchange found here is entirely consistent with our previous study.

Conclusions

Rates of hydrogen exchange comprising olefin insertion, C−C bond rotation, and β-hydrogen elimination have been measured for a series of group 5 *ansa*-niobocene or -tantalocene ethylene hydride complexes. The data indicate that both the steric bulk and the placement of cyclopentadienyl substituents have large effects on the energy barrier for hydrogen exchange. Exchange rates decrease by 3 orders of magnitude as the steric bulk is increased for those metallocenes with unsymmetrical substitution: the transition-state structure becomes more crowded as ethylene moves toward the hydride on the more sterically hindered side of the metallocene wedge. However, the ground-state structure can be destabilized by placing steric bulk on both sides of the metallocene wedge, resulting in a large enhancement in exchange rate. The exchange rate is 3 orders of magnitude larger for niobocenes with a single [$SiMe_2$] ansa bridge; however, little rate enhancement is observed for a complex with two [$SiMe_2$] bridges. The density functional calculations agree with this trend and suggest that the electron population shifts from the ground state to the transition state is the most favorable for the singly linked complex: hence, the fastest observed exchange rate.

Experimental Section

General Considerations. All air- and moisture-sensitive compounds were manipulated using standard vacuum line and Schlenk techniques or in a drybox under a nitrogen atmosphere as described previously.[19] Argon and dinitrogen gases were purified by passage over columns of MnO on vermiculite and activated molecular sieves. Toluene-d_8 was distilled from sodium benzophenone ketyl. NMR spectra were recorded on a Varian Inova or Unity^{+} 500 MHz spectrometer (^{1}H, 500.13 MHz; ^{13}C, 125.77 MHz) or a Varian Mercury 300 MHz spectrometer (^{1}H, 300.07 MHz; ^{13}C, 75.45 MHz).

Magnetization Transfer Experiments and Line Shape Analysis Experiments. For both types of experiments, the niobocene ethylene hydride samples were dissolved in toluene-d_8 and flame-sealed in NMR tubes under 700 Torr of argon at −78 °C. Reaction temperatures were determined by measuring the peak separation of an ethylene glycol or methanol standard before and after the experiments. For the line shape analysis, spectra were recorded in 10 °C increments for 40−50 °C when the hydride resonance began to broaden. This broadening was simulated using gNMR.[20] Magnetization transfer spectra were obtained by using a DANTE pulse sequence.[21] Relaxation times (T_1) for the resonances of interest were measured at each temperature before the magnetization transfer experiment using the inversion recovery method. The magnetization transfer data were fitted using the program CIFIT to obtain rate constants.[22] The reported rate constants for the elementary chemical processes of insertion followed by C−C bond rotation, k, were calculated by multiplying the exchange rate

(19) Burger, B. J.; Bercaw, J. E. In *Experimental Organometallic Chemistry*; Wayda, A. L., Darensbourg, M. Y., Eds.; ACS Symposium Series 357; American Chemical Society: Washington, DC, 1987; Chapter 4.

(20) Budzelaar, P. H. M. gNMR for Macintosh, Version 3.6; Cherwell Scientific, Oxford, U.K., 1992−1996.

(21) Morris, G. A.; Freeman, R. *J. Magn. Reson.* **1978**, *29*, 433−462.

(22) Bain, A. D.; Cramer, J. A. *J. Magn. Reson.* **1996**, *118A*, 21−27.

constant (obtained by line shape analysis or magnetization transfer), k_{ex}, by a statistical factor (1.5) according to the relationship

$$k_{ex} = (2/3)k$$

This statistical factor is necessary because, on average, after insertion and C−C bond rotation, the same hydrogen returns to niobium or tantalum one-third of the time.

Computational Methods. Calculations were performed using density functional methods of the Amsterdam Density Functional Package (Versions ADF99.02 and ADF2000.02). The generalized gradient approximation method was employed, using the local density approximation of Vosko, Wilk, and Nusair[23] together with nonlocal exchange corrections by Becke[24] and nonlocal correlation corrections by Perdew.[25] Type IV basis sets used triple-ξ accuracy sets of Slater type orbitals, with a single polarization function added to main-group atoms. The cores of the atoms were frozen up to 1s for C, 2p for Si, and 3d for Nb. First-order relativistic corrections were made to the cores of all atoms. Relativistic corrections were made using the ZORA (Zero Order Relativistic Approximation) formalism.

Reaction pathways were modeled by stepping a reaction coordinate through a sequence of fixed values and allowing the other structural parameters to optimize to a minimal energy.

All local minima and transition states were characterized by frequency calculations.

Fragment calculations were carried out to elucidate the trends in the electronic structure on an orbital basis. The fragments used were the $NbCp^R_2$ unit and the C_2H_4, H, and C_2H_5 units with geometries identical with those that they have in the optimized structure of the molecule.

Acknowledgment. This work has been supported by the USDOE Office of Basic Energy Sciences (Grant No. DE-FG03-85ER13431) and Exxon Chemicals America. L.J.A. thanks the National Science Foundation for a predoctoral fellowship. We thank Dr. Nick Rees and Dr. Jeffrey Yoder for assistance with NMR experiments and Dr. Deanna Zubris for preparation of the tantalocene complex.

OM0206296

(23) Vosko, S. H.; Wilk, L.; Nusair, M. *Can. J. Phys.* **1980**, *58*, 1200−1211.
(24) Becke, A. D. *Phys. Rev., A* **1988**, *38*, 3098−3100.
(25) (a) Perdew, J. P. *Phys. Rev., B* **1986**, *33*, 8822−8824. (b) Perdew, J. P. *Phys. Rev., B* **1986**, *34*, 7046.